THE JOURNAL OF PHYSICAL CHEMISTRY B

Article

pubs.acs.org/JPCB

Multinuclear NMR Studies on Translational and Rotational Motion for Two Ionic Liquids Composed of BF_4 Anion

Kikuko Hayamizu,*[,†] Seiji Tsuzuki,[†] Shiro Seki,[‡] and Yasuhiro Umebayashi[§]

[†]National Institute of Advanced Industrial Science and Technology, AIST Tsukuba Center 2, Tsukuba 305-8568, Japan

[‡]Central Research Institute of Electric Power Industry, Komae, Tokyo 201-8511, Japan

[§]Graduate School of Science and Technology, Niigata University, 8050, Ikarashi, 2-no-cho, Nishi-ku, Niigata City, 950-2181, Japan

Supporting Information

ABSTRACT: Two ionic liquids (ILs) based on the BF_4^- anion are studied by ^1H, ^{11}B, and ^{19}F NMR spectroscopy by measuring self-diffusion coefficients (D) and spin−lattice relaxation times (T_1). The cations are 1-ethyl-3-methylimidazolium (EMIm) and 1-butyl-3-methylimidazolium (BMIm). Since two NMR nuclei (^{11}B and ^{19}F) of BF_4^- exhibit narrow lines and high sensitivity, the ^{11}B and ^{19}F NMR measurements of D_{BF4} and $T_1(BF_4)$ were performed in a wide temperature range. The temperature-dependent behaviors of $T_1(^{19}F)$ and $T_1(^{11}B)$ were remarkably different, although the values of $D_{BF4}(^{19}F)$ and $D_{BF4}(^{11}B)$ almost agreed. Since the Arrhenius plots of T_1's for ^1H, ^{19}F, and ^{11}B exhibited T_1 minima, the correlation times $\tau_c(^1H)$, $\tau_c(^{19}F)$, and $\tau_c(^{11}B)$ were evaluated. The D(cation) and $D(BF_4)$ were plotted against $1/\tau_c(^1H)$ and $1/\tau_c(^{19}F)$, respectively, and the relationships between translational and rotational motion are discussed. The translational diffusion of the cations is related to molecular librational motion and that of BF_4 is coupled with reorientational motion. The $\tau_c(^{11}B)$ derived from ^{11}B T_1 can be attributed to a local jump. From the plots of the classical Stokes−Einstein (SE) equation, the empirical c values, which were originally derived by theoretical boundary conditions, were estimated for each ion. The empirical $c(BF_4)$ was about 4.4_5, while the c values of the cations were smaller than 4.

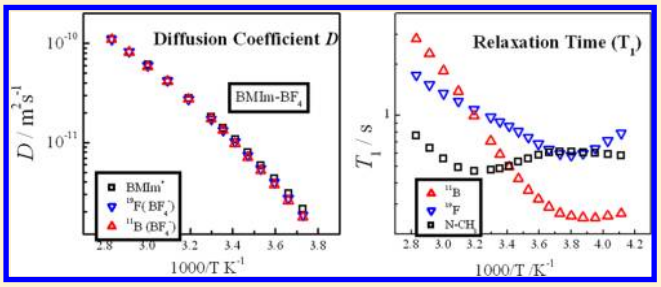

1. INTRODUCTION

Room-temperature ionic liquids (RTILs, ILs) are composed of cations and anions, and a very large number of combinations have been synthesized and studied. BF_4^- is one of the most popular anions, and many papers have been published for ILs composed of BF_4^- on the basis of experimental data such as density, viscosity, heat capacity, thermal measurements, and so forth.[1−11] The translational diffusion coefficients of BF_4^- and various cations have been published,[1,3,12,13] and spectroscopic studies have been performed over a wide frequency range for ILs containing BF_4^-.[14−20] Liquid structures of BF_4^--based ionic liquids have also been studied by means of X-ray diffraction techniques.[21−23] Molecular orbital (MO) calculations and molecular dynamics (MD) simulations have been carried out for BF_4-based ILs.[24−27] We have studied the translational diffusion and molecular motion of anions and cations for several ILs by measuring self-diffusion coefficient (D) and spin−lattice relaxation time (T_1) by multinuclear magnetic resonance (NMR) spectroscopy.[28−32] The D values for individual ions were determined from pulsed-gradient spin−echo (PGSE) NMR measurements. The correlation times of molecular local motion were calculated from temperature-dependent T_1 data, where the anions were bis(fluoromethylsulfonyl)amide ($TFSA^-$) and bis(fluorosulfonyl)amide (FSA^-). The BF_4^- anion has magnetically active nuclei of ^{10}B, ^{11}B, and ^{19}F. The easily accessible nuclei ^{11}B and ^{19}F give relatively sharp NMR spectral lines for BF_4^- in ILs. It is therefore possible to measure D and T_1 for BF_4^- from the ^{11}B and ^{19}F resonances, simultaneously. Furthermore, BF_4^- has tetrahedral symmetry and its molecular motion is expected to be different from that of $TFSA^-$ and FSA^-.

In the present study, two BF_4-based ILs, 1-ethyl-3-methylimidazolium (EMIm) and 1-butyl-3-methylimidazolium (BMIm) tetrafluoroborate, were studied by ^1H NMR for the cations and ^{11}B and ^{19}F NMR for the BF_4^- anion. The physical constants for these ILs have been published and summarized in the ionic liquids database.[33] In this paper, we present newly measured D values of the cations and BF_4^- as well as viscosity (η) and density (ρ) of the two ILs. Since the correlation times of τ_c(H) for the cations and τ_c(F) and τ_c(B) for the BF_4^- can be estimated from T_1(H), T_1(F), and T_1(B), respectively, the relationships between the translational and rotational motion will be discussed. It is noted that the D values obtained by the PGSE NMR method correspond to the translational movement of species under study.

In our previous papers, using the classical SE relation, we have estimated the constant c as an empirical parameter originally related to the boundary conditions for four cations,

Received: June 22, 2012
Revised: August 9, 2012
Published: August 21, 2012

EMIm, 1,2-dimethyl-3-propylimidazolium (DMPIm), *N*-methyl-*N*-propylpyrrolidinium (P_{13}) and *N*,*N*-diethyl-*N*-methyl-*N*-(2-methoxyethyl)ammonium (DEME) and the anions $TFSA^-$ and FSA^-. These values were smaller than 4, and deviated from the theoretically predicted values of between 4 (stick condition) and 6 (slip condition). In the present study, the plots of the SE relation afforded good linearity between D and $1/\eta$. Although the cations in this study gave values smaller than 4, similar to $EMIm^+$, $DMPIm^+$, P_{13}^+, and $DEME^+$, the value c of BF_4^- was about 4.4_5 in the range of theoretical values.

2. EXPERIMENTAL SECTION

2.1. Sample Preparation. EMIm-BF_4 and BMIm-BF_4 of high purity grade were purchased from Kanto Chemical Co., Inc. (Tokyo). For the NMR measurements, the samples were placed into a 5 mm NMR microtube (BMS-005J, Shigemi, Tokyo) to a height of 5 mm and flame-sealed.

2.2. Viscosity and Density Measurements. The samples were dried in a vacuum chamber at 323 K for more than 48 h and stored in a dry argon-filled glovebox before measurements. Viscosity η (mPas) and density ρ (g cm^{-3}) measurements were carried out using a thermo-regulated SVM3000G2 Stabinger-type viscosity and density/specific gravity meter (Anton Paar). The measurements were performed during cooling from 353 to 283 K with a stopper to avoid any moisture and air contamination.

2.3. NMR Measurements. All NMR spectra were measured on a Tecmag Apollo spectrometer equipped with a 6.4 T wide bore magnet using a JEOL PFG probe and controlled by a JEOL console. The T_1 measurements were performed using the inversion recovery (180°-τ-90°-Acq.) sequence. The ^1H, ^{19}F, and ^{11}B NMR spectra were measured at frequencies of 270.2, 254.2, and 86.7 MHz, respectively.

A modified Hahn spin−echo-based sequence incorporating a gradient pulse in each period (PGSE) was used to measure the diffusion coefficient. The echo attenuation E is related to the experimental variables and the diffusion coefficient D by

$$E = \exp[-\gamma^2 g^2 \delta^2 D(\Delta - \delta/3)] \quad (1)$$

where g is the strength of the gradient pulse of duration δ and Δ is the interval between the leading edges of the gradient pulses.[34,35] Δ defines the time scale in the diffusion measurement, and in a homogeneous system, D should be independent of Δ. A single exponential diffusion plot following eq 1 indicates free diffusion. Above ambient temperature, diffusion measurements are more prone to convection artifacts leading to Δ dependence of the measured diffusion coefficient (a larger apparent D for a longer Δ),[36] and hence D values measured with short Δ were adopted. At lower temperatures, the apparent D value is dependent on Δ and becomes larger for shorter Δ, which is opposite to the convection effects. In lower temperatures, we measured D values with longer Δ and confirmed that the same D values were obtained at different Δ values. Under the conditions described above, $D_{BF4}(^{19}F)$ and $D_{BF4}(^{11}B)$ were in agreement. At the lower temperatures, we found that $D_{BF4}(^{19}F) \geq D_{BF4}(^{11}B)$ for shorter Δ, where the apparent D value increased for the shorter Δ. Similarly, we observed that in the lower temperatures the apparent $D(^1H)$ values became larger for shorter Δ and the protons in the different positions exhibited slightly different D values. Experimentally, these effects have been measured for highly viscous ILs.[32] We took reasonable values for D without Δ- and signal-dependences observed in the longer Δ period. The errors estimated were less than 5%. It is noted that we did not observe any Δ-dependent D for neutral squalane ($C_{30}H_{62}$) ($D = 6.7 \times 10^{-12}$ m^2 s^{-1} at 273 K). The temperature range for the diffusion measurements was 353 to 253 K for EMIm-BF_4 and 353 to 268 K for BMIm-BF_4. The T_1 measurements were performed from 353 K to the lower temperature at which either heavy line-broadening or sample freezing was observed.

3. RESULTS

3.1. Density. Linear temperature dependences of the density are shown in Figure 1 for EMIm-BF_4 and BMIm-BF_4,

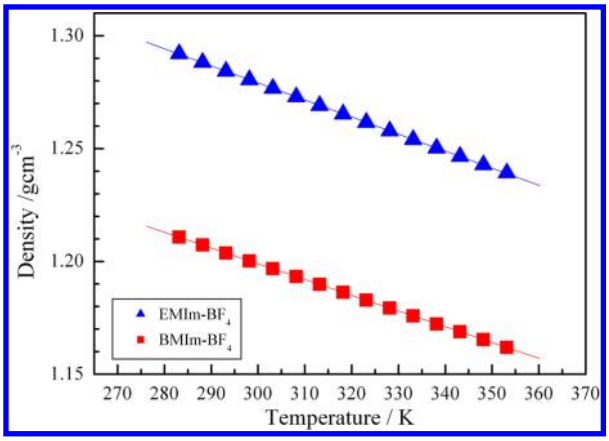

Figure 1. Temperature dependence of the density for EMIm-BF_4 (triangle) and BMIm-BF_4 (square).

which have molecular weights of 198.0 and 226.0 g mol^{-1}, respectively. The density EMIm-BF_4 was larger than BMIm-BF_4. The numerical data for the densities are given in Table S1 in Supporting Information (SI). The temperature dependences were analyzed for the density ρ against temperature T (K) as $\rho = b - aT$ and the fitting parameters a and b are also given in Table S2. At 303 K, the densities were 1.277 and 1.197 g cm^{-3} for EMIm-BF_4 and BMIm-BF_4, respectively. The comparison of the present work and literature data is given in Figure S1.

3.2. Viscosity. The temperature dependence of the viscosity η is shown in Figure 2a. Arrhenius plots for η^{-1} (fluidity) are shown in Figure 2b. The numerical data are given in Table S3. The plots were well fitted by the VFT equation $\eta^{-1} = \eta_0^{-1} \exp(-B/(T - T_o))$ and the fitted parameters are given in Table S4. At 303 K, the viscosities of EMIm-BF_4 and BMIm-BF_4 were 31.0 and 81.5 mPas, respectively. The comparison of the present work and literature data is given in Figure S2.

3.3. ^1H, ^{11}B, and ^{19}F NMR Spectra. The ^1H NMR spectra of EMIm and BMIm did not exhibit any impurity signals as shown in Figure S3. The ^{19}F spectrum of BF_4 consisted of large $^{11}BF_4$ signal and small $^{10}BF_4$ signal, and the latter was located a little lower field side. Since BF_4 includes three magnetic nuclei such as ^{10}B (spin $I = 3$, natural abundance about 20%), ^{11}B ($I = 3/2$, about 80%), and ^{19}F ($I = 1/2$, 100%), the ^{19}F spectrum is affected by ^{10}B and ^{11}B nuclei through J-coupling and isotope shift. In Figure S4, the ^{19}F and ^{11}B spectral patterns of BF_4^- are shown for $LiBF_4$ dissolved in D_2O and BF_4^- in $EMImBF_4$.

3.4. Self-Diffusion Coefficients. The temperature dependence of the cation diffusion coefficients D_{EMIm} and D_{BMIm} was measured by ^1H resonance and anion diffusion coefficient D_{BF4} was measured by ^{11}B and ^{19}F resonances. Arrhenius plots of the D_{cation} and D_{BF4} are shown in Figure 3 for EMIm-BF_4 and

dx.doi.org/10.1021/jp306146s | J. Phys. Chem. B 2012, 116, 11284−11291

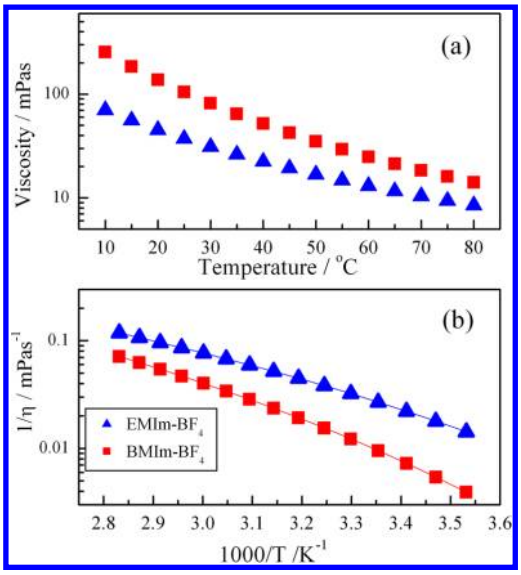

Figure 2. (a) Viscosity plotted versus temperature and (b) Arrhenius plots of $1/\eta$ for EMIm-BF_4 (triangle) and BMIm-BF_4 (square).

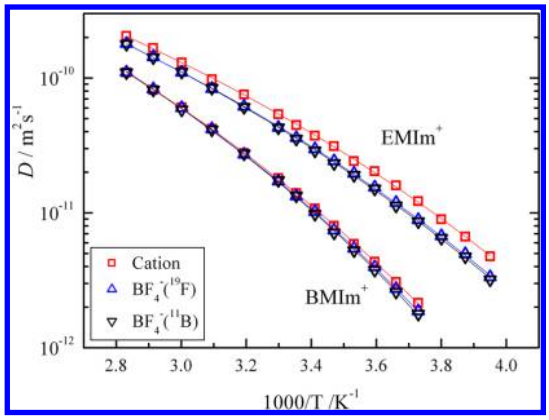

Figure 3. Arrhenius plots of diffusion coefficients for D_{cation} (square), D_{BF4}(F) (up-triangle), and D_{BF4}(B) (down-triangle) measured by ^{1}H, ^{19}F, and ^{11}B NMR, respectively, for EMIm-BF_4 and BMIm-BF_4.

BMIm-BF_4. Although the two values of D_{BF4} measured by ^{11}B and ^{19}F resonances exactly agreed at high temperatures, D_{BF4}(F) was slightly larger than D_{BF4}(B) at low temperatures. The fitted lines by the VTF equation $D = D_0 \exp(-B/(T - T_o))$ are shown. The numerical data of the temperature dependence of D_{cation} and D_{BF4} for EMIm-BF_4 and BMIm-BF_4 are given in Tables S5 and S6, respectively. The fitting parameters of the VFT equation are also given in Table S7.

The classical SE relation connects the value of D for a diffusing particle of radius a with the bulk viscosity η as

$$D = \frac{kT}{c\pi\eta a} \tag{2}$$

where k is the Boltzmann constant and the constant c theoretically ranges between 4 and 6 for slip and stick boundary conditions, respectively.[37,38] The D values are plotted against $kT/\pi\eta$ for (a) D_{BF4} and (b) D_{cation}'s for the two ILs in Figure 4 by assuming that c is an empirical parameter. When we presume that the SE relation is valid, the slope of each line corresponds to the inverse of $c \times a$. The experimental values of $c \times a$ are summarized in Table 1, where the errors estimated for the linear plots were less than 1%. Clearly, the classical SE

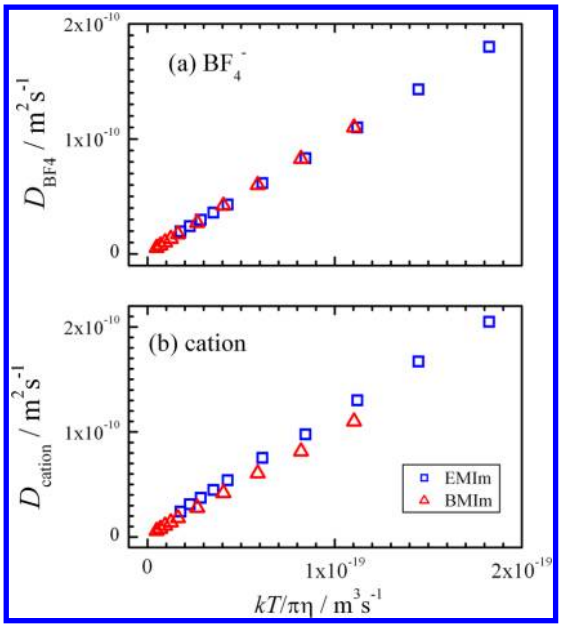

Figure 4. Diffusion coefficients were plotted vs $kT/\pi\eta$ for (a) BF_4^- and (b) cations.

Table 1. SE Relationships for Each Ion in EMIm-BF_4 and BMIm-BF_4

ion	counter ion	$c \times a$ /nm	a /nm	V /nm^3	c
EMIm	BF_4	0.912 ± 0.006	0.303[a]	0.1165	3.0_1
BMIm		1.017 ± 0.006	0.330[b]	0.1505	3.0_8
BF_4	EMIm	1.028 ± 0.004	0.229[c]	0.0503	4.4_9
	BMIm	1.006 ± 0.004			4.3_9

[a]Ref 31. [b]Ref 39. [c]Ref 40.

consistency given in eq 2, i.e., $D \propto 1/\eta$, can be used to clarify the physical meaning between the translational ion diffusion and bulk viscosity in the present ILs. Here, we assume that the van der Waals radius calculated from the van der Waals volume can be used as the radius of diffusing ions as given in Table 1. The c values calculated for the two cations in the present study were between 3.0 and 3.1, and the c values of BF_4 were 4.5 and 4.4.

3.5. Spin−lattice Relaxation Times T_1 for ^{1}H, ^{19}F, and ^{11}B NMR. The values of T_1 for ^{11}B and ^{19}F of BF_4 and for ^{1}H of N−CH_3 as well as α-CH_2 in the butyl chain in BMIm-BF_4 are plotted against temperature in Figure 5. Clearly, each T_1 exhibited a minimum value. Since spin $I = 1/2$ for ^{1}H and ^{19}F resonances, the dipolar−dipolar relaxation mechanism predominantly determines the ^{1}H and ^{19}F T_1. The classical Bloembergen, Purcell, and Pound (BPP) equation (eq 3)[41] can be applied to obtain the correlation time τ_c for the motion of dipoles.

$$\frac{1}{T_1} = C\left(\frac{\tau_c}{1 + \omega_0^2\tau_c^2} + \frac{4\tau_c}{1 + 4\omega_0^2\tau_c^2}\right) \tag{3}$$

where ω_0 is the observe frequency (rad s^{-1}), and τ_c is the correlation time of the dipolar interaction. C in eq 3 is written as

$$C = \frac{3}{10}\gamma^4\hbar^2 \sum_j \frac{1}{r_j^6} \tag{4}$$

dx.doi.org/10.1021/jp306146s | J. Phys. Chem. B 2012, 116, 11284−11291

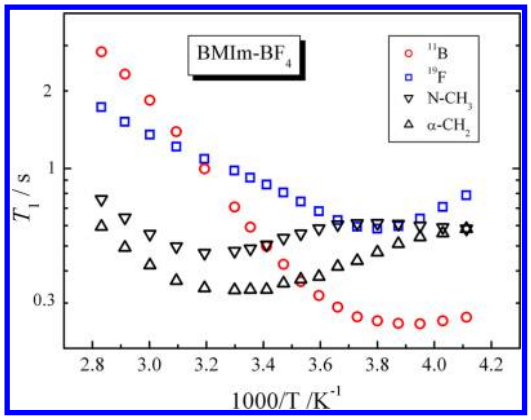

Figure 5. Arrhenius plots of T_1 of ^{1}H, ^{11}B, and ^{19}F NMR for BMIm-BF_4.

where γ is the magnetogyric ratio of ^{1}H or ^{19}F, r is the atomic distance between protons (^{1}H) or fluorine atoms (^{19}F), τ_c is the correlation time of the dipolar interaction, and the summation index j is over all interacting dipoles. Owing to the term in brackets in eq 3, T_1 is minimum when $\omega_o\tau_c = 2\pi\nu_0\tau_c = 0.616$. In the present experiments, ν_0(H) and ν_0(F) are 270.2 and 254.2 MHz, and at the minimum temperature, the τ_c(H) and τ_c(F) are 3.63 and 3.86 × 10^{-10} s (363 and 386 ps), respectively.

Since spin I = 3/2 for ^{11}B, a quadrupolar interaction can be assumed as the dominant relaxation mechanism. Here, we assume the quadrupolar BPP equation[42] for the ^{11}B relaxation process

$$\frac{1}{T_1} = \frac{\omega_q^2}{50}\left(\frac{\tau_c}{1+\omega_0^2\tau_c^2} + \frac{4\tau_c}{1+4\omega_0^2\tau_c^2}\right) \quad (5)$$

where $\omega_q = 2\pi\nu_q$ (rad s^{-1}) is the quadrupole coupling constant for the ^{11}B nuclei. At the minimum T_1, $\omega_0\tau_c = 2\pi\nu_0\tau_c = 0.616$ and $\nu_0(^{11}B)$ = 86.7 MHz giving $\tau_c(^{11}B)$ = 1.13 × 10^{-9} s (1.13 ns). The calculated ν_q (^{11}B) from the T_1 minimum values were about 43 and 39 kHz for BF_4^- in BMIm-BF_4 and EMim-BF_4, respectively. These values are similar to the value of ν_q (^{7}Li) (40−55 kHz) for Li^+ ion in polymer electrolytes, in which the translational motion of the lithium ions can be assumed as relaxation mechanism.[43]

3.6. Cation Motion (^{1}H NMR). The temperature dependence of T_1 for all the protons of BMIm-BF_4 and τ_c(H) calculated using eq 3 are shown in Figure S5. The activation energies calculated from the τ_c(H) are given in Table 2 together with the temperature range for the linear plots. Similarly, the T_1 of ^{1}H for EMIm-BF_4 exhibited minima and the activation energies are included in Table 2. It is clear that the activation energies became smaller as the protons of the alkyl chains approached the terminal positions.

As described in our previous papers,[28−32] the motion of cations, which results in the Arrhenius plots having minimum value of T_1, is mainly due to isotropic reorientational motion. Local faster intramolecular motions such as the rotation of CH_3 and segmental motions of chain of CH_2 are averaged out in the condensed state. The correlation time τ_c can be written as

$$\frac{1}{\tau_c} = \frac{1}{\tau_o} + \frac{1}{\tau_s} \quad (6)$$

where τ_o and τ_s are the correlation times for the isotropic reorientational and residual local intramolecular motion, respectively. The longest τ_c is most likely to be the closest value for the overall reorientational motion. In Figure S5(b), τ_c for N−CH_3 had the largest value above 278 K, which corresponds to the slowest motion. We assume that $\tau_c(NCH_3)$ is the correlation time of the reorientational motion for BMIm. Similarly, N−CH_3 of EMIm had the largest τ_c value. The comparison of the behaviors of the T_1 of ^{1}H resonance for N−CH_3 of EMIm and BMIm is shown in Figure S6. The τ_c values obtained at 303 K are summarized in Table 3, where the τ_c of EMIm is much smaller (faster motion) than that of BMIm.

Table 3. τ_c(^{1}H), τ_c(^{19}F), and τ_c(^{11}B)/ps at 303 K

	EMIm-BF_4	BMIm-BF_4
N−CH_3	166	450
α-CH_2	141	340
β-CH_2/CH_3	88	230
δ-CH_2	-	178
t-CH_3	-	158
^{19}F	-	119
^{11}B	68	192

The overall isotropic molecular correlation time τ_2 is related to the viscosity η by the Stokes−Einstein-Debye (SED) relation as

$$\tau_2 = \frac{V\eta}{kT} \quad (7)$$

where V is the effective molecular volume.[44,45] This relation was originally proposed for rotational time of a solute in a solvent of shear viscosity η. The values of τ_2 calculated using the viscosity and the van der Waals volume in Table 1 are plotted against temperature in Figure 6, in addition to the values of τ_c (cation) obtained from the ^{1}H T_1 of NCH_3. In

Table 2. Activation Energies/kJ mol^{-1} for τ_c(^{1}H), τ_c(^{19}F), and τ_c(^{11}B)

		EMIm-BF_4	BMIm-BF_4
^{1}H NMR	N-CH_3	21.4 ± 0.2 (263−353K)	22.9 ± 0.6 (288−353 K)
	α-CH_2	20.7 ± 0.2 (263−353 K)	19.4 ± 0.4 (273−353 K)
	β-CH_2/CH_3	16.1 ± 0.1 (238−353 K)	18.8 ± 0.3 (243−353 K)
	γ-CH_2	-	18.5 ± 0.2 (243−353 K)
	t-CH_3	-	15.3 ± 0.2 (243−353 K)
^{19}F NMR	BF_4	7.8 ± 0.2 (248−298 K)[a]	25.6 ± 0.2 (248−283 K)
		10.8 ± 0.1 (303−353 K)[a]	11.5 ± 0.2 (288−353 K)
^{11}B NMR	BF_4^-	26.1 ± 0.5 (233−303 K)	13.4 ± 0.5 (228−273 K)
		16.2 ± 0.4 (313−353K)	26.9 ± 0.4 (273−353 K)

[a]Estimated from T_1(^{19}F).

dx.doi.org/10.1021/jp306146s | J. Phys. Chem. B 2012, 116, 11284−11291

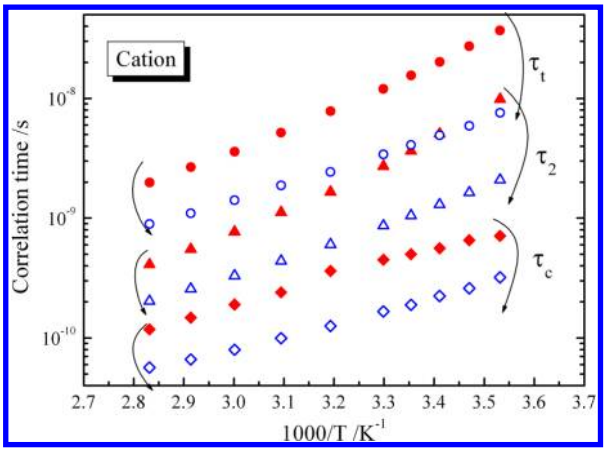

Figure 6. Temperature dependences of τ_t (circle), τ_2 (triangle), and τ_c (diamond) for the cations. Solid red: $BMIm^+$; and open blue: $EMIm^+$.

NMR relaxation theory, the translational correlation time can be defined as $\tau_t = 2a^2/D$ following Abragam,[46] where a is the radius of the diffusing particle. Additionally, the values of τ_t are included in Figure 6. Clearly, $\tau_t > \tau_2 > \tau_c$ for each cation and the correlation times of BMIm are longer than those of EMIm. In this study, we adopted the simplest models for translational and rotational molecular motion without considering the molecular shapes, mutual ionic interactions, and so forth over wide range of temperatures.

To understand the relationship between ion translational diffusion and the molecular motion, D_{cation} values were plotted against the rate of molecular motion $1/\tau_c$(cation) in Figure 7.

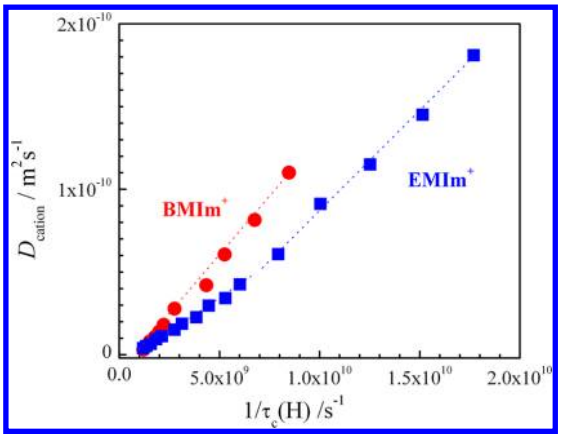

Figure 7. Values of D_{cation} plotted against $1/\tau_c(^1H)$ for $EMIm^+$(red circle) and $BMIm^+$(blue square).

Almost linear and bilinear relations were obtained for the $BMIm^+$ and $EMIm^+$, respectively, and the slopes have the unit of m^2. The square-root value of the slope for $BMIm^+$ was 0.12_0 nm in the entire temperature range measured. It was 0.11 nm above 313 K and 0.09 nm below 313 K for $EMIm^+$. The value obtained from the slope affords the estimation for a distance during a rotational flip of each cation. $EMIm^+$ flips more frequently with slightly shorter distance rather than $BMIm^+$.

3.7. BF_4^- Motion. BF_4^- includes two easily accessible magnetic nuclei, ^{11}B and ^{19}F. Although $D(^{11}B)$ and $D(^{19}F)$ had similar values in Figure 3, T_1 values of ^{19}F and ^{11}B for the same BF_4 are quite different as shown in Figure 5. The Arrhenius plots of ^{19}F T_1 for the BF_4^- of the two ILs are shown in Figure S7(a). BMIm-BF_4 gave the ^{19}F T_1 minimum and afforded $\tau_c(^{19}F)$ using eq 3 as shown in Figure S7(b). Two activation energies for the $\tau_c(^{19}F)$ obtained from a bilinear plot are given in Table 2. The activation energy for BF_4^- obtained ^{19}F T_1 of EMIm-BF_4 is also included. The $\tau_c(^{19}F)$ value for BMIm-BF_4 at 303 K is given in Table 3. The activation energies of $\tau_c(^{19}F)$ for BF_4^- are clearly smaller than those of τ_c(cation, for N–CH_3) above 288 K in Table 2. This suggests that the rotational motion of BF_4^- can be activated more easily than that of the cations owing to the smaller ion size and a tetrahedral symmetrical structure.

The values of D_{BF4} are plotted against the rate $1/\tau_c(^{19}F)$ in Figure 8 for BMIm-BF_4. A good bilinear correlation was

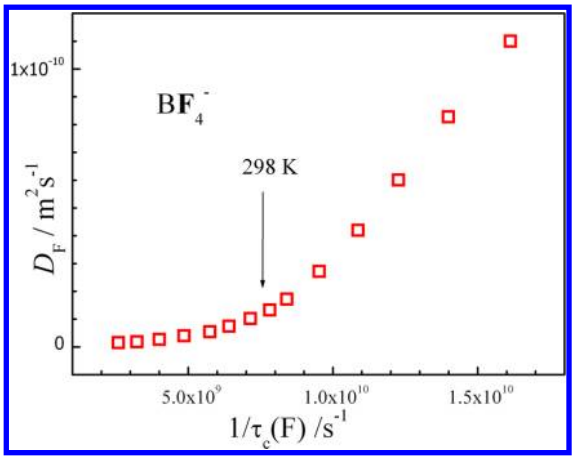

Figure 8. Plot of D_{BF4} versus $1/\tau_c(^{19}F)$ for BMIm-BF_4.

obtained, where the value of the smaller slope at lower temperatures corresponds to 0.04 nm and the steeper slope at higher temperatures gave the values of 0.11 nm. These values can be assumed to translational distances during a single rotational motion. The distance for BF_4^- resembles those for the cations at higher temperatures in Figure 7, while it is much shorter in BF_4^- in the lower temperature region.

The Arrhenius plots of the ^{11}B T_1 and the $\tau_c(^{11}B)$ based on the T_1 minimum are plotted for the two BF_4^- in Figure S8. The activation energies calculated for the bilinear region for the $\tau_c(^{11}B)$ are given in Table 2. From the tetrahedral symmetry of BF_4^-, we assumed that the translational motion more significantly affects the ^{11}B relaxation process rather than the rotational motion. Since T_1 is reflected by one flip of dipole (^{19}F–^{19}F) or a quadrupole (^{11}B), the time derived from T_1 corresponds to a single motion. Comparing the activation energies in various temperatures in Table 2, we presume that, in the lower temperature region, the rotational motion (^{19}F) of BF_4^- in EMIm-BF_4 is carried out with smaller activation energy than the translation motion (^{11}B). In the higher temperature region, the relation is similar but the difference of the activation energies became smaller. The BF_4^- in BMIm-BF_4 behaves in different ways that the activation energy was larger in rotational motion (^{19}F) rather than translational motion (^{11}B) in the lower temperatures, while in the higher temperature region, rotational motion (^{19}F) is easily activated rather than translational motion (^{11}B).

Under the assumption that ^{11}B relaxation occurs by mainly translational movement, the $\tau_c(^{11}B)$ corresponds to a single jump of BF_4^-. The average diffusion distance $\sim 10^{-6}$ m is calculated by $(6D\Delta)^{1/2}$ during the period Δ ($\sim 10^{-2}$ s) in eq 1 and experimental D. The activation energies for the D_{BF4} in

dx.doi.org/10.1021/jp306146s | J. Phys. Chem. B 2012, 116, 11284–11291

Figure 3 were calculated to be 25.9 ± 0.3 (293−353 K) and 34.6 ± 0.6 (283−353 K) kJ mol^{-1} for EMIm-BF_4 and BMIm-BF_4, respectively. The larger activation energies for D_{BF4} compared with those of the $\tau_c(^{11}B)$ are reasonable. The average distance for one-jump translational diffusion can be assumed for $\bar{r} = [6D_{BF4}\tau_c(^{11}B)]^{1/2}$, and the calculated values are plotted against temperature in Figure 9. When the temperature

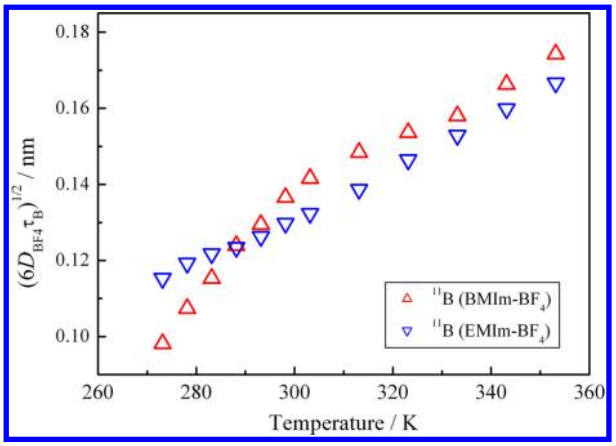

Figure 9. Temperature dependence of mean distance for one flip of BF_4^- derived from D_{BF4} and $\tau_c(^{11}B)$.

increased from 273 to 353 K, the values of $\bar{r}$ increased from approximately 0.1 to 0.17 nm for the BF_4^- in BMIm-BF_4. This is comparable with the distance of during one flip obtained from the relation of D_{BF4} and $1/\tau_c(^{19}F)$ in Figure 8, which were calculated to be 0.04 and 0.11 nm in low and high temperatures, respectively. The behavior of the average distance of BF_4^- in EMIm-BF_4 was different from that of BF_4^- in BMIm-BF_4 and linearly increased as the temperature increased. Unfortunately, a flip distance of BF_4^- in EMIm-BF_4 could not be estimated from the relation of D_{BF4} and $1/\tau_c(^{19}F)$, because the ^{19}F T_1 minimum was not observed in the Arrhenius plot.

To understand the relationships among the translational correlation time τ_t calculated from D_{BF4}, the rotational correlation time τ_2 calculated from the viscosity and ion size, the rotational correlation time $\tau_c(^{19}F)$ and local translational correlation time $\tau_c(^{11}B)$, the temperature dependences of these correlation times were plotted for BMIm-BF_4 as shown in Figure 10. It was found that $\tau_t > \tau_2 > \tau_c$ ($\tau_c(^{19}F)$ and $\tau_c(^{11}B)$),

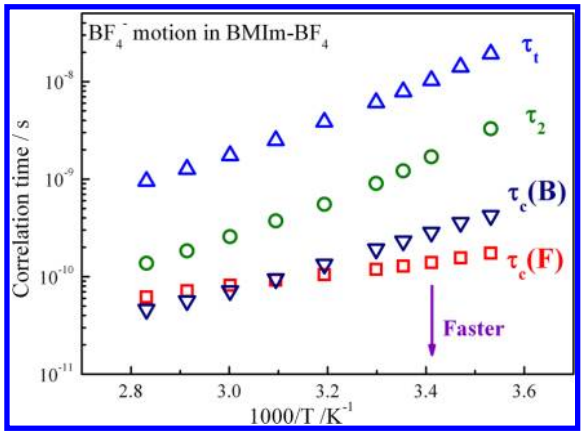

Figure 10. Correlation times of τ_t, τ_2, $\tau_c(^{19}F)$, and $\tau_c(^{11}B)$ plotted against temperature for BMIm-BF_4.

similar to the correlation times for the cations in Figure 6. A comparison between $\tau_c(^{19}F)$ and $\tau_c(^{11}B)$ suggests that the BF_4^- rotational motion ($\tau_c(^{19}F)$) is slower than the local jump $\tau_c(^{11}B)$ in the high temperatures, while it is opposite in the low temperature. When the temperature is low, the rotational motion occurs more frequently than the translational one-jump. It is not certain that the $\tau_c(^{19}F)$ and $\tau_c(^{11}B)$ represent purely rotational and translational motion, respectively. The rotational and translational motion may be coupled in the local motion of BF_4^-.

4. DISCUSSION

4.1. Relationships between *D* and *η*. Although D is generally proportional to $1/\eta$ in ILs, the exact application of SE relation (eq 2) to ILs is difficult. We have proposed empirical c values (theoretically between 4 and 6) of each ion in ILs from the experimental values of D and η in the temperature range between 283 and 353 K using an ionic radius calculated by MO methods. In this study, the empirical c values for BF_4 ($c(BF_4)$) were 4.4 and 4.5 and larger than the c(TFSA) of 3.5−3.8 for four ILs and the c(FSA) of 2.8−3.1 in two ILs.[30] The values of c(cation) in this study were about 3.1. As included in our previous studies, approximate values of c(EMIm) were 3.1 in EMIm-BF_4, 2.8 in EMIm-TFSA, and 2.5 in EMIm-FSA. The values of c(cation) were between 2.5 and 3.2 hitherto obtained,[32] and smaller than 4. Although the empirical c values were calculated from the ion size, the shape of ions was not accounted. Note that the ions having smaller c values undergo intramolecular motion. If the actual radius of diffusing ions were smaller in ILs, the c value would become larger, and vice versa. Theoretical interpretation of empirical c values is needed in the future.

4.2. Molecular Motion. The D values of BF_4^- for the movement of the center of mass were almost the same for the ^{11}B and ^{19}F resonances, except for a short period Δ at low temperatures. The diffusion phenomena in ILs are coupled with molecular reorientational motion described above by the D versus $1/\tau_c$. To interpret the isotropic reorientational motion of the cations and the BF_4^- anion, the flip amplitudes were estimated under the assumption that τ_2 corresponds to 360° rotation, while τ_c is the time for librational motion. The amplitude of the angle is plotted against temperature in Figure 11. $EMIm^+$ and $BMIm^+$, which include an imidazolium ring,

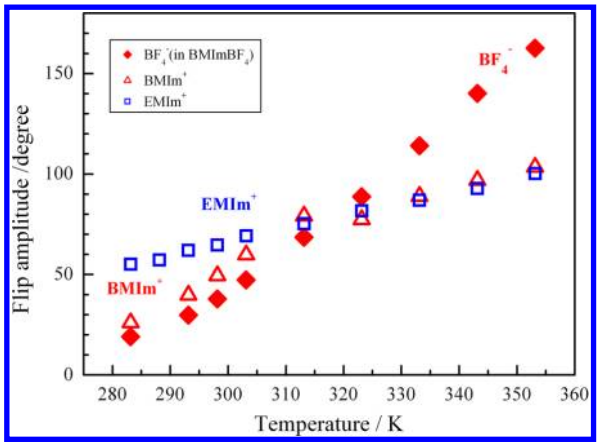

Figure 11. Flip amplitude of librational motion plotted against temperature for the $EMIm^+$ (open square) and $BMIm^+$ (open triangle) and that of rotational motion for BF_4^- (solid diamond) in BMIm-BF_4.

dx.doi.org/10.1021/jp306146s | J. Phys. Chem. B 2012, 116, 11284−11291

exhibited similar flip amplitudes above ambient temperature, while at lower temperatures, the flip amplitude of $BMIm^+$ decreased significantly. The flip amplitude of BF_4^- was very small at lower temperatures in spite of the small ion size. At higher temperatures, the flip amplitude rapidly increased with the increase of temperature and approached a π-flip. Strong interactions around BF_4^- are suggested to occur in lower temperatures which prevent a rapid rotational flip. Actually, the activation energies of $\tau_c(^{19}F)$ in Table 3 clearly indicate that the BF_4^- rotational motion is activated much easier in high temperatures (about 12 kJ mol^{-1}) than in low temperatures (about 26 kJ mol^{-1}).

4.3. Translational Distance during a Flip of an Ion. The jump distances during the molecular flip of the cations are about 0.08 and 0.11−0.12 nm at lower and higher temperatures, respectively, and are smaller than their van der Waals radii (0.3 to 0.33 nm). Thus, the rotational and translational motion is strongly suggested to be coupled, and it would be difficult to strictly apply a rigid particle model for diffusion, particularly in the lower temperatures. The translational distances of BF_4^- during a flip motion obtained from $D(BF_4)$ and $1/\tau_c(^{19}F)$ were 0.04 and 0.11 nm at lower and higher temperatures, respectively. The averaged distance during a molecular flip of BF_4^- derived from $D(BF_4)$ and $\tau_c(^{19}F)$ increased from about 0.1 to 0.2 nm from 273 to 353 K. Since the van der Waals radius of BF_4^- is 0.23 nm, each jump takes place within the ion size. A short displacement is accompanied by small-angle librational or rotational motion of both the cations and the BF_4^- anion in the present ILs.

We described the interactions between rotational and translational motion from experimental data for the BF_4-based ILs. Similarly, ionic rotation and translation dynamics study for PF_6^- having octahedral symmetry in BMIm-PF_6 have been made by MD calculation.[47] In viscous ILs, translational motion may be deeply influenced by molecular rotational motion.

5. CONCLUSION

Two BF_4-based ILs with cations of $EMIm^+$ and $BMIm^+$ were studied by ^1H, ^{11}B, and ^{19}F NMR by measuring the T_1 and self-diffusion coefficients. The relationships between D and $1/\eta$ were interpreted using the classical SE relation and the empirical constant c was derived for each ion. The c values of the cations were small, about 3.1, while the c values of the BF_4 were about 4.4$_5$. The correlation times τ_c(cation), and $\tau_c(^{19}F)$ and $\tau_c(^{11}B)$ for BF_4^- were evaluated from the Arrhenius plots of $T_1(^1H)$, $T_1(^{19}F)$, and $T_1(^{11}B)$ having the T_1 minima, respectively, and the relationships between D and $1/\tau_c$ showed that the diffusion distance during a flip is shorter than the radius of the ions. Our results indicate that the translational and rotational motion of ions in ILs is strongly coupled.

■ ASSOCIATED CONTENT

Ⓢ Supporting Information

Numerical data of density, viscosity, and anion and cation diffusion coefficients for EMIm-BF_4 and BMIm-BF_4. Comparison of density and viscosity of the present work and literature data. ^1H, ^{19}F, and ^{11}B spectral patterns. Arrhenius plots of T_1 and correlation time τ_c for ^1H, ^{19}F, and ^{11}B resonances. This information is available free of charge via the Internet at http://pubs.acs.org.

■ AUTHOR INFORMATION

Corresponding Author

*E-mail: hayamizu.k@aist.go.jp.

Notes

The authors declare no competing financial interest.

■ REFERENCES

(1) Noda, A.; Hayamizu, K.; Watanabe, M. *J. Phys. Chem. B* **2001**, *105*, 4603−4610.
(2) Fredlake, C. P.; Crosthwaite, J. M.; Hert, D. G.; Aki, S. N. V. K.; Brennecke, J. F. *J. Chem. Eng. Data* **2004**, *49*, 954−964.
(3) Tokuda, H.; Ishii, K.; Susan, MABH; Tsuzuki, S.; Hayamizu, K.; Watanabe, M. *J. Chem. Phys. B* **2006**, *110*, 19593−19600.
(4) Harris, K. R.; Kanakubo, M.; Woolf, L. A. *J. Chem. Eng. Data* **2007**, *52*, 2425−2430.
(5) Pensado, A. S.; H. Pádua, A. A.; Comuñas, M. J. P.; Fernández, J. *J. Phys. Chem. B* **2008**, *112*, 5563−5574.
(6) Sánches, L. G.; Espel, J. R.; Onink, F.; Meindersma, C. W.; de Haan, A. B. *J. Chem. Eng. Data* **2009**, *54*, 2803−2812.
(7) Mokhtarani, B.; Sharifi, A.; Mortaheb, H. R.; Mirzaei, M.; Mafi, M.; Sadeghian, F. *J. Chem. Thermodyn.* **2009**, *41*, 323−329.
(8) Ghatee, M. H.; Moosavi, F.; Zolghadr, A. R.; Jahromi, R. *Ind. Eng. Chem. Res.* **2010**, *49*, 12696−12701.
(9) Sanmamed, Y. A.; Navia, P.; González-Salgado, D.; Troncoso, J.; Romaní, L. *J. Chem. Eng. Data* **2010**, *55*, 600−604.
(10) Fletcher, S. I.; Sillars, B.; Hudson, N. E.; Hall, P. J. *J. Chem. Eng. Data* **2010**, *55*, 778−782.
(11) Stoppa, A.; Zech, O.; Kunz, W.; Buchner, R. *J. Chem. Eng. Data* **2010**, *55*, 1768−1773.
(12) Hayamizu, K.; Aihara, Y.; Nakagawa, H.; Nukuda, T.; Price, W. S. *J. Phys. Chem. B* **2004**, *108*, 19527.
(13) Sangoro, J.; Iacob, C.; Serghei, A.; Naumov, S.; Galvosas, P.; Kärger, J.; Wespe, C.; Bordusa, F.; Stoppa, A.; Hunger, J.; Buchner, P.; Kremer, F. *J. Chem. Phys.* **2008**, *128*, 214509−214513.
(14) Dahl, K.; Sando, G. M.; Fox, D. M.; Sutto, T. E.; Owrutsky, J. C. *J. Chem. Phys.* **2005**, *123*, 084504−084514.
(15) Umebayashi, Y.; Fujimori, T.; Sukizaki, T.; Asada, M.; Fujii, K.; Kanzaki, R.; Ishiguro, S. *J. Phys. Chem. A* **2005**, *109*, 8976−8982.
(16) Heimer, N. E.; Del Sesto, R. E.; Meng, Z.; Wilkes, J. S.; Carper, W. R. J. *Mol. Liq.* **2006**, *124*, 84−95.
(17) Nishi, T.; Iwahashi, T.; Yamane, H.; Ouchi, Y.; Kanai, K.; Seki, K. *Chem. Phys. Lett.* **2008**, *455*, 213−217.
(18) Hunger, J.; Stoppa, A.; Schrödle, S.; Hefter, G.; Buchner, R. *ChemPhysChem* **2009**, *10*, 723−733.
(19) Khara, D. C.; Samanta, A. *Phys. Chem. Chem. Phys.* **2010**, *12*, 7671−7677.
(20) Hayamizu, K.; Tsuzuki, S.; Seki, S. *Magn. Reson. Chem.* **2011**, *49*, 6−8.
(21) Kanzaki, R.; Mitsugi, T.; Fukuda, S.; Fujii, K.; Takeuchi, M.; Soejima, Y.; Takamura, T.; Yamaguchi, T.; Umebayashi, Y.; Ishiguro, S. *J. Mol. Liq.* **2009**, *147*, 77−82.
(22) Takamuku, T.; Kyoshoin, Y.; Shimomura, T.; Kittaka, S.; Yamaguchi, T. *J. Phys. Chem. B* **2009**, *113*, 10817−10824.
(23) Kanakubo, M.; Aizawa, T.; Nanjo, H.; Kameda, Y.; Amo, Y.; Usuki, T. *Fluid Phase Equilib.* **2010**, *297*, 183−186.
(24) Lynden-Bell, R. M.; Popolo, M. D. *Phys. Chem. Chem. Phys.* **2006**, *8*, 949−954.
(25) Bagno, A.; D'Amico, F.; Saielli, G. *J. Phys. Chem. B* **2006**, *110*, 23004−23006.
(26) Borodin, O. *J. Phys. Chem. B* **2009**, *113*, 11463−11478.
(27) Sun, H.; Qiao, B.; Zhang, D.; Liu, C. *J. Phys. Chem. A* **2010**, *114*, 3990−3996.
(28) Hayamizu, K.; Tsuzuki, S.; Seki, S. *J. Phys. Chem. A* **2008**, *112*, 12027−12036.
(29) Hayamizu, K.; Tsuzuki, S.; Seki, S.; Ohno, Y.; Miyashiro, H.; Kobayashi, Y. *J. Phys. Chem. B* **2008**, *112*, 1189−1197.
(30) Hayamizu, K.; Tsuzuki, S.; Seki, S.; Fujii, K.; Suenaga, M.; Umebayashi, Y. *J. Chem. Phys.* **2010**, *113*, 194505−194513.

(31) Hayamizu, K.; Tsuzuki, S.; Seki, S.; Umebayashi, Y. *J. Chem. Phys.* **2011**, *135*, 084505−08416.
(32) Hayamizu, K. *Translational and Rotational Motions for TFSA-Based Ionic Liquids Studied by NMR Spectroscopy*, Handy, S. T. (Ed.), (InTech, 2011) . http://www.intechopen.com/articles/show/title/translational-and-rotational-motions-for-tfsa-based-ionic-liquids-studied-by-nmr-spectroscopy
(33) http://ilthermo.boulder.nist.gov/ILThermo/mainmenu.uix
(34) Stejskal, E. O.; Tanner, J. E. *J. Chem. Phys.* **1965**, *42*, 288−293.
(35) Tanner, J. E. *J. Chem. Phys.* **1970**, *52*, 2523−2527.
(36) Hayamizu, K.; Price, W. S. *J. Magn. Reson.* **2004**, *167*, 328−333.
(37) Tyrrell, H. J. V.; Harris, K. R. *Diffusion in Liquids: A Theoretical and Experimental Study*; Butterworth: London, 1984.
(38) Price, W. S. *NMR Studies of Translational Motion, Principles and Applications*; Cambridge University Press: Cambridge, 2009.
(39) Ue, M.; Murakami, A.; Nakamura, S. *J. Electrochem. Soc.* **2002**, *149*, A1385−A1388.
(40) Ue, M. *J. Electrochem. Soc.* **1996**, *143*, L270−L272.
(41) Traficante, D. D. *Relaxation: An Introduction, in Encyclopedia of Nuclear Magnetic Resonance*, Grant, M. D., Harris, R. K., Eds.; Wiley: New York, 1996; Vol. *6*, p 3988.
(42) Werbelow, L. G. *Relaxation Theory for Quadrupolar Nuclei, in Encyclopedia of Nuclear Magnetic Resonance*, Grant, M. D., Harris, R. K., Eds.; Wiley: New York, 1996; Vol. *6*, p 4092.
(43) Hayamizu, K.; Aihara, Y.; Price, W. S. *J. Chem. Phys.* **2000**, *113*, 4785−4793.
(44) Mazza, M. G.; Giovambattista, N.; Stanley, H. E.; Starr, F. W. *Phys. Rev. E* **2007**, *76*, 031203−031215 and references therein..
(45) Köddermann, T.; Ludwig, R.; Paschek, D. *ChemPhysChem* **2008**, *9*, 1851−58.
(46) Abragam, A. *The Principles of Nuclear Magnetism*; Oxford University Press: London, 1961; p 302.
(47) Li H.; Kobrak, M. N. *J. Chem. Phys.* **2009**, *1*